International Journal of Heat and Fluid Flow 30 (2009) 939–949

Contents lists available at ScienceDirect

International Journal of Heat and Fluid Flow

journal homepage: www.elsevier.com/locate/ijhff

Accurate heat transfer measurements using thermochromic liquid crystal. Part 1: Calibration and characteristics of crystals

V.U. Kakade, G.D. Lock *, M. Wilson, J.M. Owen, J.E. Mayhew [1]

Department of Mechanical Engineering, University of Bath, Bath, BA2 7AY England, United Kingdom

ARTICLE INFO

Article history:
Received 26 August 2008
Received in revised form 22 December 2008
Accepted 21 April 2009
Available online 19 May 2009

Keywords:
Heat transfer
Thermochromic liquid crystal
Calibration

ABSTRACT

Encapsulated thermochromic liquid crystal (TLC) can accurately measure surface temperature in a variety of heat transfer and fluid flow experiments. Narrow-band TLC, where the colour changes over a temperature range of ~1 °C, can be used to determine surface temperature within an uncertainty of 0.1 °C. Wide-band TLC, typically active over 5–20 °C, allow the possibility of mapping surface temperature distributions. In part 1 of this two-part paper, an extensive set of calibrations for narrow-band and wide-band TLC is reported. This generic study provides insight into the importance and influence of the various factors governing the colour–temperature relationship. These governing effects include the variation in optical path, the spectrum of the illumination source, the lighting and viewing angles, the differences between cooling or heating cycles (hysteresis), the variation with the number of heating or cooling cycles (aging) and how this varies with TLC film thickness. Two narrow-band crystals are also specifically calibrated for application to experiments on a transparent disc rotating at high speed (~5000 rpm). Part 2 of this paper describes how these accurately-calibrated crystals were used to measure the transient surface temperature on, and heat transfer to, a rotating disc.

1. Introduction

Thermochromic liquid crystal (TLC) has become a practical and accurate means of measuring surface temperature. Usually a thin film of TLC microcapsules is sprayed onto a solid material and the colour response allows the surface temperature to be measured accurately. A great advantage is that TLC can cover the complete surface, enabling the measurement of global temperature distributions. Unlike thermocouples or other intrusive devices, TLC creates no local disturbance error; unlike infrared detectors, no special windows (such as germanium) are required for studying the heat transfer in internal flows – windows made from glass, acrylic or polycarbonate provide adequate optical access.

The temperature-sensing ability arises from the molecular structure within the TLC, which occurs within a temperature range corresponding to a transition between solid and liquid states. In this liquid crystal phase, molecules lose positional order (becoming fluid) but retain orientation order (retaining the optical properties of crystalline solids). This transitional temperature range may be wide (5–20 °C) or narrow (~1 °C). Many texts on the molecular structure of these materials are available (e.g. Bahadur, 1998), and Ireland and Jones (2000) provide a good summary of how two important structures (nematic and cholesteric) relate to optical activity pertinent to the sensing of temperature. In essence, TLC is characterised by a helical molecular structure, the periodicity of which is a function of temperature. When illuminated with white light, the liquid crystal selectively reflects monochromatic light with a wavelength equal to the pitch of the helical structure. The wavelength of the reflected light decreases with increasing temperature so that the colour changes from red, through the visible spectrum to blue. Typical time constants for the colour changes near room temperature have been measured to be ~3 ms (Ireland and Jones, 1986). The reader is referred to Kasagi et al. (1989) for a general description of liquid crystals, their physical and chemical properties, and other characteristics (including colour and imaging processing.)

Liquid crystals are organic compounds which degrade when exposed to ultraviolet radiation but this degradation is reduced by microencapsulation, which encloses the TLC in polymer spheres <0 μm in diameter. Microcapsules of different liquid crystal formations can be mixed together to produce films with multiple colour ranges. Commercial micro-encapsulated TLC may be purchased in a water-based slurry and is generally applied to flat or curved surfaces using an air-brush spray. The thickness of the TLC film must be controlled carefully: a layer that is too thin produces poor colour, while a layer that is too thick may create a significant and undesirable change of temperature across the film. Brilliant colours can be achieved by using a black background, usually air-brush sprayed paint or ink.

* Corresponding author. Tel.: +44 1225 386854.
E-mail address: ensgdl@bath.ac.uk (G.D. Lock).
[1] Present address: Rose-Hulman Institute of Technology, IN, USA

0142-727X/$ - see front matter © 2009 Elsevier Inc. All rights reserved.
doi:10.1016/j.ijheatfluidflow.2009.04.007

Nomenclature for Parts 1 and 2

a	rotor inner radius
b	rotor outer radius
Bi	Biot number based on film thickness = $h\delta x/k$
c	specific heat
c_j	weighting term in exponential series
c_w	non-dimensional mass flow rate ($=\dot{m}/\mu b$)
C	cycle number
$g\ (\beta,\ \beta_\tau)$	slow-transient solution of Fourier's equation = $g(\beta, \lambda)$
h	heat transfer coefficient ($=q_w/(T_{aw}-T_w)$)
H	hue
k	thermal conductivity
q_w	heat flux from air to wall
m	number of terms in exponential series
$\dot{m}$	mass flow rate
P	uncertainty (95% confidence estimate)
Re_ϕ	rotational Reynolds number ($=\rho\Omega b^2/\mu$)
r	radius
r_p, r_b	radii of pre-swirl nozzles and receiver holes
R	probe recovery factor
RGB	red, green, blue intensities
s	rotor–stator separation distance
S_c	seal clearance
t	time
T	temperature
$T_a(t)$	total-temperature of air
$T_{aw}(t)$	adiabatic-wall temperature
T_e	copper block temperature
T_{tc}	temperature measured by thermocouple
$T_w(t)$	surface temperature of wall
V	velocity
β	non-dimensional heat transfer coefficient = $(h\sqrt{t/\kappa})$
β_τ	non-dimensional heat transfer coefficient =$(h\sqrt{\tau/\kappa})$
β_p	swirl ratio ($=V_\phi/\Omega r$)
δx	effective thickness of TLC film
κ	thermal diffusivity of plate = ρck
ζ	normalised temperature for calibration
θ	relative lighting and viewing angle
Θ	non-dimensional temperature in solution to Fourier's eq. = $\frac{T_w-T_0}{T_{aw,\infty}-T_0}$
λ	non-dimensional time = $\sqrt{t/\tau}$
λ_T	turbulent flow parameter ($=c_w\mathrm{Re}_\phi^{-0.8}$)
μ	dynamic viscosity
ρ	density
τ	time constant
Φ_h^*	amplification parameter for uncertainty in h
Ω	angular velocity of rotor

Subscripts

0	value at $t = 0$
j	term in exponential series
M	median value
min	minimum value
o	overall
R, G, B	red, green, blue
Φ	circumferential direction

In experimental heat transfer, one of the more demanding issues related to liquid crystals is the colour–temperature relationship, and any quantitative application of TLC requires an accurate calibration. The TLC signal is generally quantified by either intensity or hue. Intensity-based image processing usually matches the peak intensity to a single temperature calibration point. Image processing based on hue, which is defined in terms of the RGB tristimulus signals, has the advantage that the hue–temperature relationship is monotonic, and hardware and software for RGB to hue conversion are readily available. There are many papers related to TLC calibration and the main factors which are pertinent to the calibration presented here are summarised as follows: acceleration due to rotation (Syson et al., 1996; Camci et al., 1998); illumination source (Behle et al., 1996; Anderson and Baughn, 2005); illumination and viewing angles (Camci et al., 1992; Farina et al., 1994; Behle et al., 1996; Sabatino et al., 2000, Chan et al., 2001); hysteresis, aging and TLC film thickness (Anderson and Baughn, 2004; Wiberg and Lior, 2004); and optical path (current study). Further details are discussed in Sections 2 and 3.

This paper describes the calibration of both wide-band and narrow-band TLC using an isothermal surface of known temperature. The research substantiates the findings of others and provides new insights into some important effects, including aging, TLC film thickness, 'optical path' and the use of a normalised temperature. Two narrow-band crystals are also specifically calibrated for application to experiments on a transparent disc rotating at high speed (~5000 rpm). The calibration accounts for acceleration due to rotation, the strobe illumination source frequency (synchronised to the disc rotation), the illumination and viewing angles, hysteresis, aging, TLC film thickness and the inherent indirect optical access. Part 2 describes how these accurately-calibrated crystals were used to measure the surface temperature on, and heat transfer to, the rotating disc in a transient experiment modelling the flow of internal cooling air in a gas turbine.

2. Calibration apparatus and method

The use of TLC in experimental heat transfer requires a quantitative relationship between colour and temperature. This section describes the calibration method used for the colour–temperature interpretation.

2.1. TLC film thickness

To reduce irreversible damage from solvents and ultraviolet radiation, the TLC was used in micro-encapsulated form. Small spherical capsules (<0 μm in diameter) were mixed with an adhesive binder and then this mixture was diluted with water. For experiments in which the analysis requires more than one type of TLC, the encapsulated crystals were combined before the water-borne emulsion was sprayed, using an airbrush, onto the polycarbonate test surface. A thin layer of black paint was used to provide contrast and enhance the colour visibility of the TLC. A single wide-band and two narrow-band TLC were used: the wide-band crystal (Hallcrest R30C5W) was active between 31 and 36 °C, and is simply denoted as the wide-band crystal; both narrow-band crystals (Hallcrest R30C1W and R40C1W) were active over 1C at approximately 30 and 40 °C, and are denoted as the 30 °C crystal and 40 °C crystal, respectively. Here the activation and clearing-point temperatures are defined as the minimum and maximum temperatures in the range where the crystal reflects light.

The thickness of the TLC film must be controlled carefully: a layer that is too thin produces poor colour, while a layer that is too thick may create a significant and undesirable change of temperature across the film. In heat transfer experiments, the film should be sufficiently thin such that the TLC temperature is (within reason) the same as the surface temperature of a semi-infinite insulator and subject to the same heat transfer history. Film thicknesses of 15, 30 and 45 μm were used in the experiments and

calibration; these thicknesses were created by spraying different volumes of TLC over a 65 × 65 mm test piece. The thinnest coat used was created by spraying 4 ml and the thickest layer obtained using 24 ml of TLC over the same area. The thickness of the TLC layers was measured using a scanning electron-microscope and a typical photograph is shown in Fig. 1. The thickness of the black paint was measured to be 5 μm. The uncertainty in all thickness measurements was 5%.

2.2. Effect of rotation

The experiments (described in Part 2) used a transparent polycarbonate rotating disc which modelled the flow of internal cooling air in a gas turbine, and the TLC was viewed through the disc using a digital video camera and strobe light synchronised to the disc frequency. The calibration of the TLC, in contrast, was conducted using a stationary copper-block apparatus which created an isothermal surface of known temperature. Rotating surfaces experience centripetal acceleration and it should be noted that Syson et al. (1996) investigated the effect of rotation on the calibration of TLC. In their experiments, the surface temperature of a rotating disc was measured simultaneously using an infra-red imager and wide-band TLC, and within the uncertainty of the measurements it was concluded that there was no significant rotational effect up to 16,000 g, where g is the acceleration due to gravity. Similar conclusions were obtained by Camci et al. (1998).

2.3. Calibration apparatus

In all calibrations, the hue of the TLC was measured as a function of temperature. The stationary calibration was performed using the copper-block apparatus shown in Fig. 2. It consists of a copper block (65 × 65 × 5 mm) mounted in Rohacell insulating foam ($k \sim 0.04\ \mathrm{Wm^{-1}\,K^{-1}}$). The block was heated electrically by a thin-film heater attached to the back face, and the temperature measured using a *K*-type thermocouple embedded in the centre of the block. This thermocouple was calibrated, along with two surface-mounted and five fast-response thermocouples used elsewhere on the experimental apparatus, over the range 20–100 °C in a Haake oil bath. The temperature of the silicone oil was measured using NPL mercury-filled thermometers with a manufacturer's specified uncertainty of 0.025 °C. The thermocouple cold junction, which was in an isothermal box at around 20 °C, was measured with a platinum resistance thermometer with an uncertainty of 0.1 °C over the range 20–65 °C. All calibration temperature measurements, denoted T_e, are referenced to the embedded thermocouple.

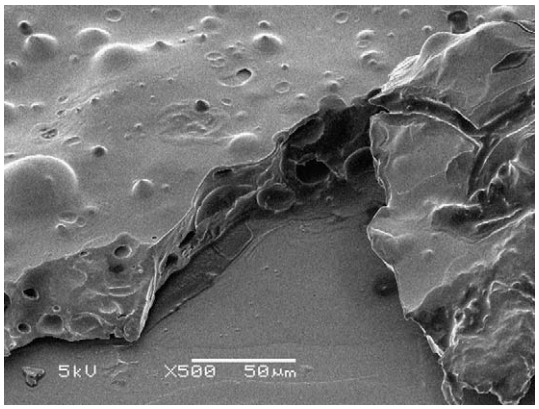

Fig. 1. Scanning electron-microscope photograph of thermochromic liquid crystal, including length scale.

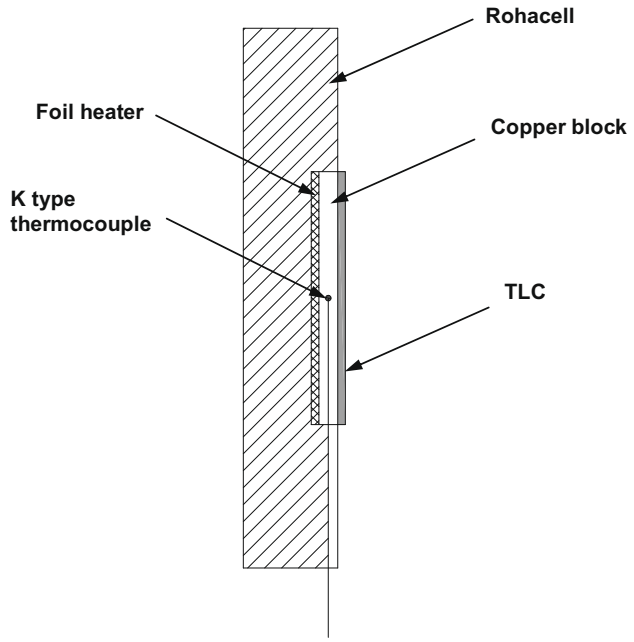

Fig. 2. Calibration apparatus using isothermal copper block.

For a *direct-view* calibration, the front surface of the copper was spray-painted with black paint prior to application of the TLC coating under test. The maximum thickness of the coating (TLC and black paint) in the current experiments was less than 60 μm. The copper block was heated at a maximum rate of 0.002 °C/s to 45 °C (upper limit of the higher-temperature crystals) where, assuming a typical thermal conductivity of $0.2\ \mathrm{Wm^{-1}\,K^{-1}}$ for the coating, the temperature drop across the coating due to radiation and free convective heat transfer to the ambient was estimated to be less than 0.1 °C. The temperature drop across the copper block itself was an order of magnitude less.

In the experiments, the crystals were viewed through the transparent polycarbonate disc with black paint sprayed over the TLC

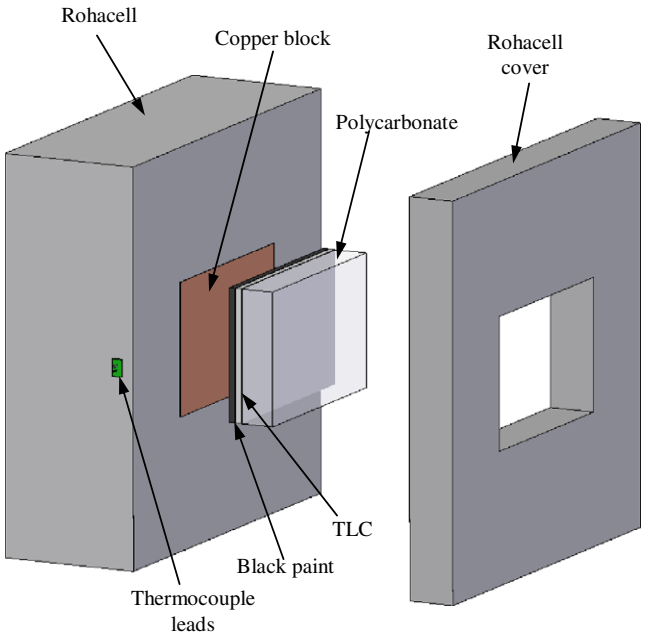

Fig. 3. Apparatus for indirect calibration.

film on the exposed side. This optical arrangement required an *indirect-view* calibration, as illustrated in Fig. 3. Here the TLC and black paint were applied to a 10 mm-thick polycarbonate test piece (the same thickness as the disc) which was bonded to the copper block surface using heat-sink compound ($k \sim 0.6\ \mathrm{Wm^{-1}\,K^{-1}}$) to ensure good thermal contact. A Rohacell cover was used to provide thermal insulation from the surroundings. Two surface-mounted thermocouples were used to ensure no significant difference in temperature between the polycarbonate surface coated with TLC and the isothermal copper block. This difference in temperature was measured to be less than 0.06 °C (which is within the uncertainty of the thermocouples) over the range of the TLC calibration, $20 < T_e < 42$ °C.

The calibration was conducted in a dark-room with the test piece illuminated by a strobe light (Chadwick Helmuth strobex lamp model 270C) operating over the range of frequencies expected in the experiments. The TLC colour display was recorded using a CCD camera (Panasonic NV-MX500) mounted perpendicular to the calibration apparatus with the light incident from a range of angles, θ, relative to the axis of camera as illustrated in Fig. 4. This off-axis lighting arrangement was chosen to minimise direct reflections from the optical windows. The camera shutter speed, aperture settings and white balance were fixed for all experiments.

2.4. Image processing

The image processing was conducted using MATLAB R2007a and its Image Processing Toolbox, and an image of the entire calibration surface contained approximately 250 × 250 pixels. Though the apparatus was designed to be isothermal, there were small variations in lighting angle and TLC thickness over the calibration surface. In order to minimise these effects, smaller 50 × 50 pixel sections in locations around the surface were selected for processing. The standard deviation in average hue from the different sections was within experimental uncertainty. Following the method of Baughn et al. (1999), the data from each section was processed using a 5 × 5 median filter (Medfit2 in MATLAB) on each of the RGB image components separately. This filter replaced the RGB values in each pixel with the median of the values within the surrounding block. The resulting RGB image was then converted to hue and averaged over each 50 × 50 pixel section. There are various definitions of hue; here the hue is determined using the formulation given by MATLAB.

3. Effects of viewing, lighting, hysteresis, aging and film thickness

The main factors which influenced the hue–temperature calibration are described in the sub-sections below. These governing effects include: the variation in optical path; the spectrum of the illumination source and how this might change with strobe frequency; the lighting and viewing angles; the differences between cooling or heating cycles (hysteresis); the variation with the number of heating or cooling cycles (aging) and how this varies with TLC film thickness.

3.1. Direct versus indirect view

The term optical path is used here to describe the differences between a direct and indirect view; for the latter, the light will pass through the transparent polycarbonate medium. Fig. 5 is a plot of hue, H, as a function of temperature measured using the embedded thermocouple, T_e. Here the 40 °C crystal is compared using a direct and indirect calibration with all other influencing factors constant (e.g. viewing and illumination angles, TLC film thickness, aging cycle).

For both the direct and indirect views, the TLC has a minimum activation temperature and the hue increases monotonically, but non-linearly, as the temperature is increased. Near the clearing-point temperature ($H > 0.7$) the TLC ceases to reflect colour and becomes transparent. There is a definite change of slope at the green-to-blue transition ($H \sim 0.38$) and the calibration is less useful above this point because the resolution decreases as $\mathrm{d}H/\mathrm{d}T$ decreases. The two calibrations have a similar shape and activation range in terms of hue and temperature. However, there is a noticeable shift of about 0.6 °C for the same value of hue. By refraction, or some other optical process, the polycarbonate medium is believed to alter the spectral content of the RGB components and consequently shift the hue. Similar effects were measured using the

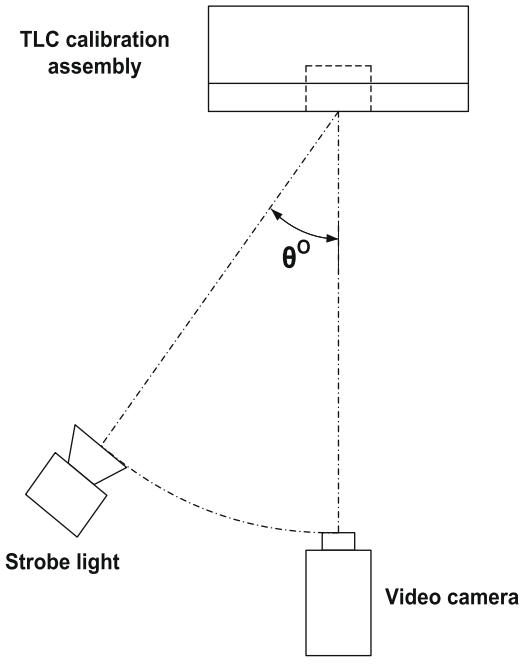

Fig. 4. Relative lighting and illumination angle for calibration.

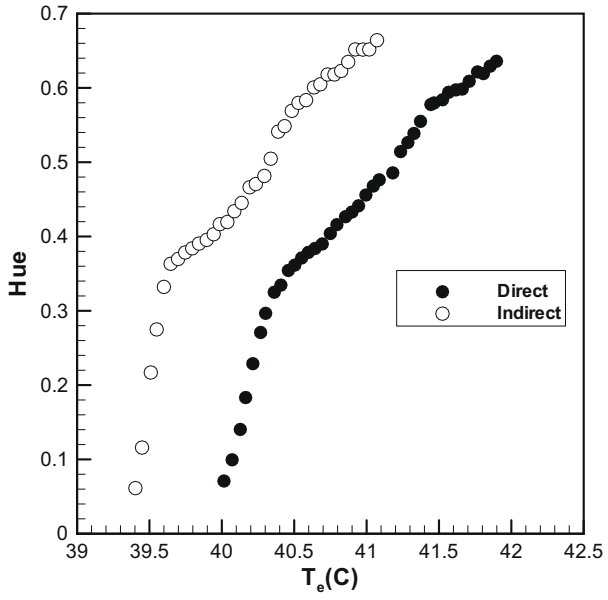

Fig. 5. Variation of hue with temperature for direct and indirect view for 40 °C crystal.

30 °C and wide-band crystals. It should be noted that these calibrations were repeatable as long as the TLC was kept below the upper clearing-point temperature; if the temperature was increased beyond this point the TLC experienced hysteresis (see Section 3.4) and aging (see Section 3.5).

3.2. Influence of strobe frequency

The spectral distribution of the illumination source will affect the TLC response, and in most TLC experiments the primary source of illumination dominates the background lighting. Anderson and Baughn (2005) examined the spectral effects of a variety of illumination sources including a tungsten, halogen and fluorescent filaments. Here all calibrations and experiments were conducted for an indirect view in a dark-room using only the strobe light as illumination. Fig. 6 shows a calibration of hue as a function of temperature for the 30 °C crystal illuminated at three frequencies, which correspond to the disc rotational speeds of 1000, 3000 and 5000 rpm used in the experiments. The measurements indicate that the spectral distribution of the strobe light does not change significantly with frequency and that the hue–temperature relationship is independent of the strobe frequency. The effects of rotational acceleration were discussed in Section 2.2.

3.3. Lighting and viewing arrangement

TLC is sensitive to the viewing and illumination angles: Farina et al. (1994), Behle et al. (1996), Sabatino et al. (2000), and Chan et al. (2001) have all reported significant shifts in the hue temperature correlations of wide-band TLC. Camci et al. (1992) reported that the effect of viewing angle (θ, see Fig. 4) with narrow-band TLC was negligible between $0 < \theta < 40$ but potentially significant at greater angles. Here the influence of viewing angle on the calibration of both narrow- and wide-band TLC has been studied. In order to match the subsequent experiments, in all cases the calibrations are for an indirect view, the TLC film thicknesses were all 45 μm and the TLC was experiencing the first heating cycle. In Fig. 4, θ is the angle between a normal view and the illumination angle. For the calibration, the illumination angle was fixed at 34° and $\theta = 20°$, 28°, 34° (to match the experiment) and 45°.

Figs. 7a and b illustrate the variation of hue with temperature using θ as a parameter (shown in the legend) for the 30 and 40 °C crystals, respectively. For the narrow-band crystals there is no significant effect at lower values of hue but the curves are observed to diverge beyond the green-to-blue transition ($H > 0.38$). The effect of the lighting/viewing arrangement might suggest the necessity of a unique calibration for each pixel in view of the camera for $H > 0.38$; although possible, this would be cumbersome in most practical situations and it was imperative to ensure that an image-wise, rather than point-wise calibration was suitable. Under each lighting arrangement, i.e. for each θ, the variation in measured hue ($0 < H < 0.7$) across a 60 mm width of the isothermal TLC surface was within the uncertainty limits. This 60 mm spacing

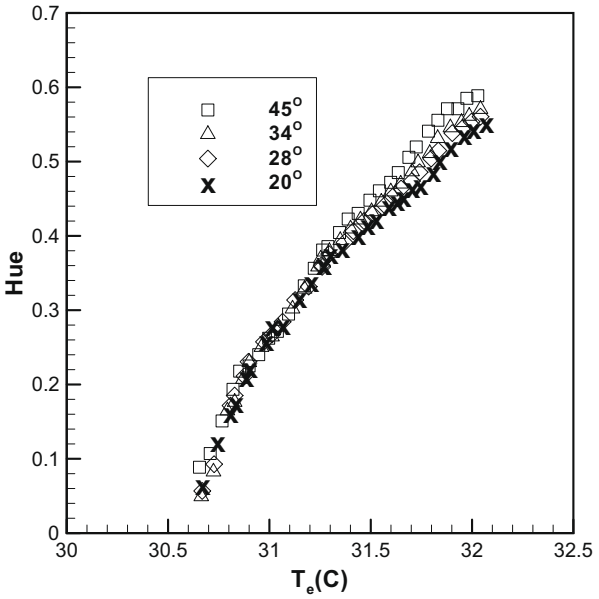

Fig. 7a. Effect of illumination angle on variation of hue with temperature for 30 °C crystal.

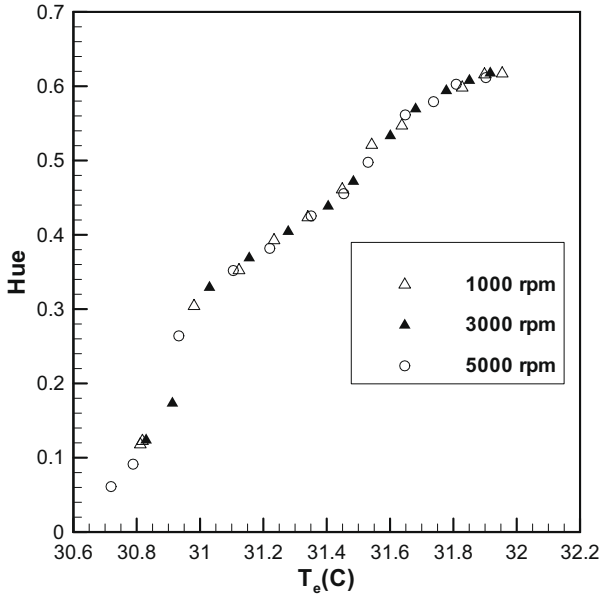

Fig. 6. Effect of strobe frequency on variation of hue with temperature for 30 °C crystal.

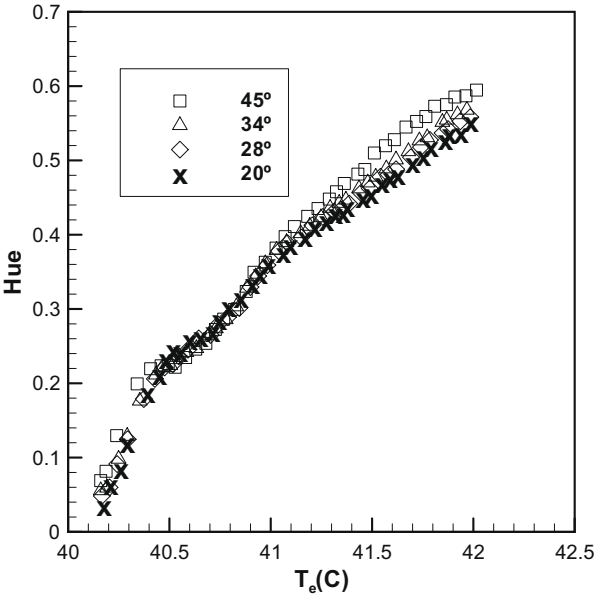

Fig. 7b. Effect of illumination angle on variation of hue with temperature for 40 °C crystal.

corresponds to an arc of 17.5° on the rotating disc used in the experimental setup (see Part 2), which was the maximum field of view used for the analysis; this 17.5° arc corresponded to a variation in lighting angle, $\theta < 2°$. Thus a unique pixel-by-pixel calibration for the narrow-band TLC was considered unnecessary.

Fig. 8a illustrates the variation of hue with temperature using θ as a parameter for the wide-band crystal. Though active over a wider range, only data for $0 < H < 0.38$ is shown. Here a significant shift in the calibration with viewing angle is observed over the entire temperature range tested. Hay and Hollingsworth (1998) suggested a normalised temperature which collapsed data from TLC with different active ranges to a single calibration curve. This concept has been extended to account for the differences in viewing angles (and in the next section hysteresis) of the wide-band TLC. Values of hue corresponding to the green and red intensity peaks, H_G and H_R, were chosen as the upper and lower extremes of the hue domain. The corresponding temperatures, T_G and T_R, were determined by the calibration curve as shown in Fig. 8b. A third temperature, T_M, is defined as the temperature at the mean hue, H_M, between H_G and H_R. The normalised temperature is defined as follows:

$$\zeta = \frac{T - T_M}{\Delta T} \tag{1}$$

where $\Delta T = T_G - T_M$ if $T > T_M$ or $\Delta T = T_M - T_R$ if $T < T_M$.

This definition of ζ allows the two halves of the calibration curve to be stretched independently about a centre, $\zeta\ (H_M) = 0$. Fig. 8c shows that the normalised temperature effectively collapses the wide-band data onto a single characteristic curve for all viewing angles over a range $-1 < \zeta < 1$. These results help simplify the quantitative response of the wide-band TLC over a range of lighting conditions and viewing angles. However, further investigation is required if a normalised temperature is to be usefully applied universally.

3.4. Hysteresis

The colour response (i.e. hue–temperature relationship) of TLC is known to depend upon whether the crystals are undergoing a cooling or heating cycle. This difference, referred to as hysteresis

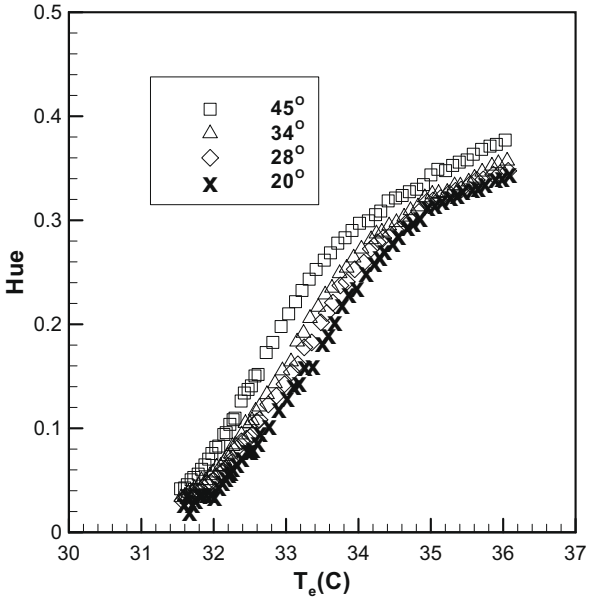

Fig. 8a. Effect of illumination angle on variation of hue with temperature for wide-band crystal.

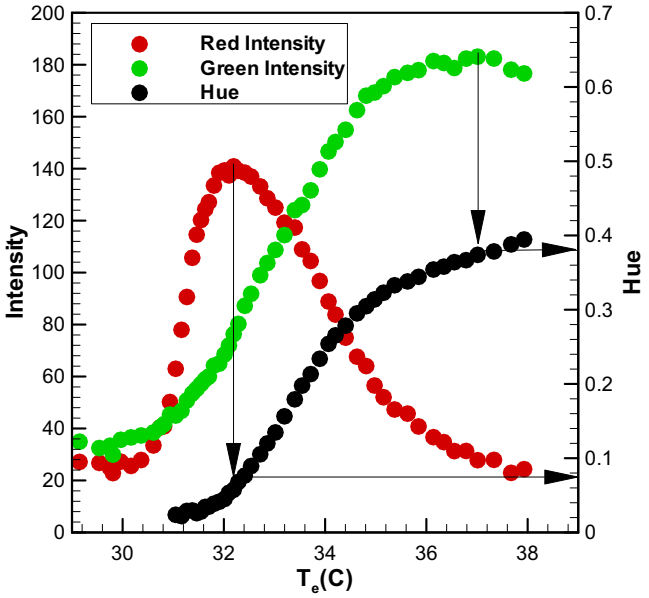

Fig. 8b. Variation of intensity and hue with temperature for wide-band crystal.

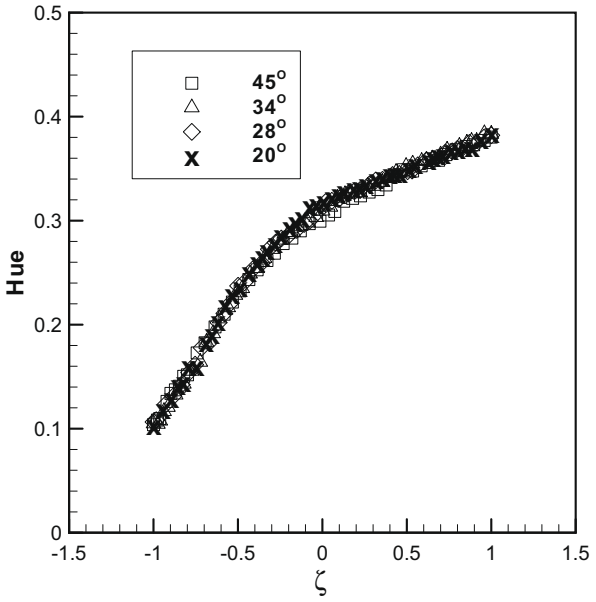

Fig. 8c. Effect of viewing angle on variation of hue with normalised temperature for wide-band crystal.

(Anderson and Baughn, 2004), can be reduced significantly if the cycle is kept below the clearing-point temperature. The TLC is observed to reset when it is cooled below the activation temperature. If the TLC temperature is raised significantly beyond the clearing-point, then the colour response can be permanently altered due to damage or aging (Sabatino et al., 2000; Wiberg and Lior, 2004). Anderson and Baughn (2004) suggested a possible explanation of the hysteresis based on the texture of the liquid crystal helical structure.

The above effects have all been observed in this study. Hysteresis was investigated using a mixture of 30 and 40 °C narrow-band TLC which was heated from 20 to 42.5 °C, a temperature just beyond the clearing-point of the 40 °C crystal. In order to match the subsequent experiments, the calibrations are for an indirect view, the TLC film thickness was 45 μm and the TLC was

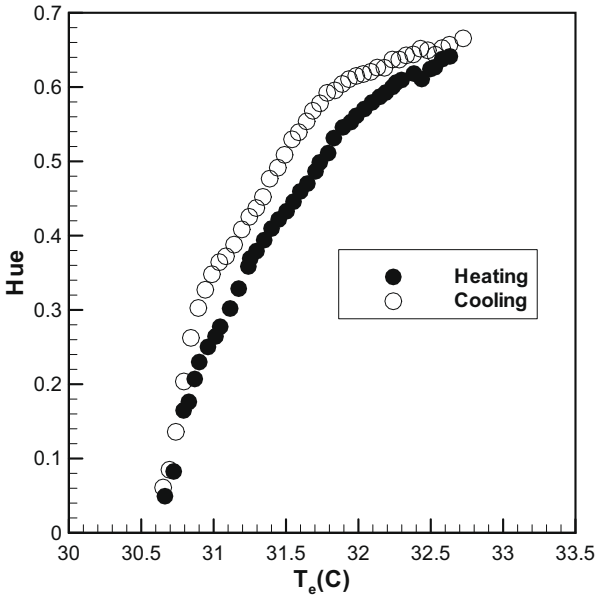

Fig. 9a. Effect of heating or cooling cycle on variation of hue with temperature for 30 °C crystal.

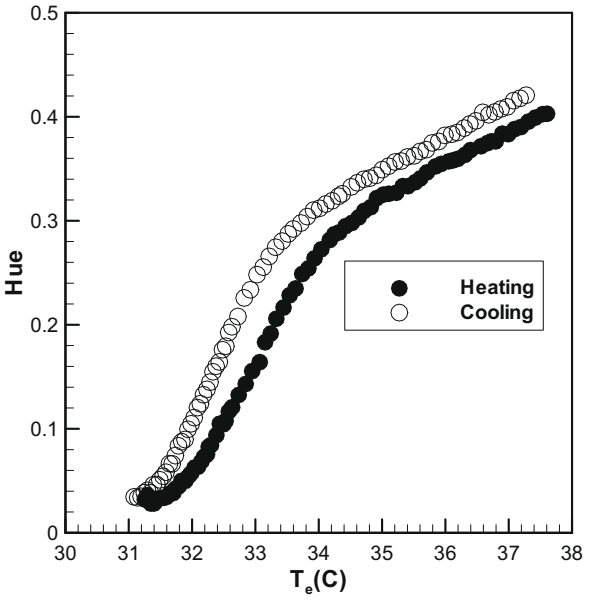

Fig. 10a. Effect of cooling or heating cycle on variation of hue with temperature for wide-band crystal.

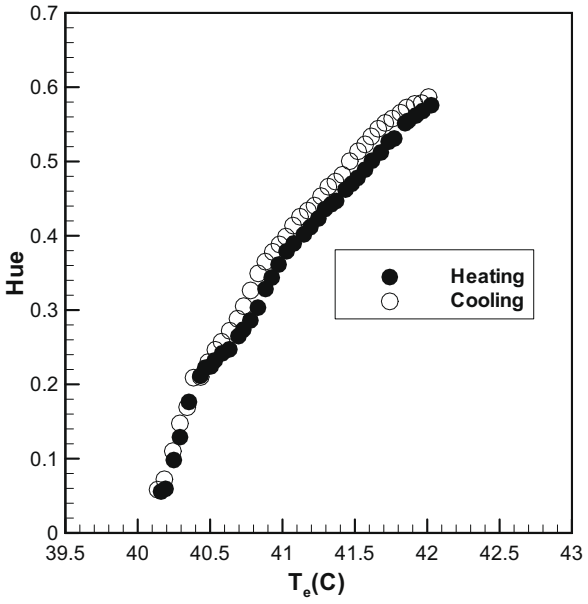

Fig. 9b. Effect of cooling or heating cycle on variation of hue with temperature for 40 °C crystal.

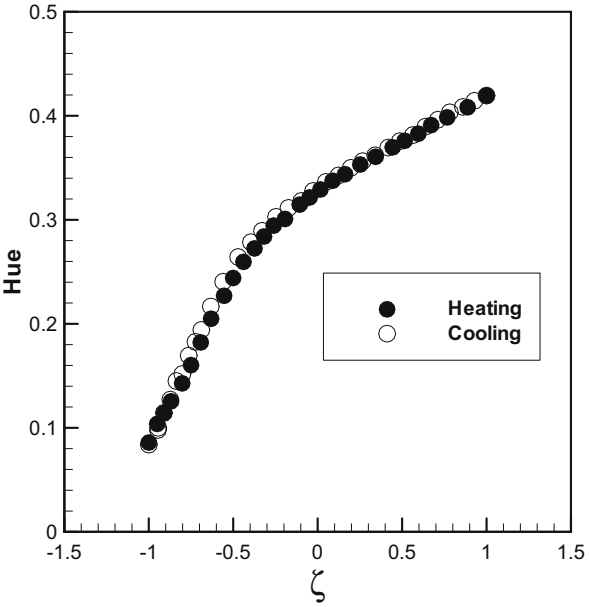

Fig. 10b. Effect of cooling or heating cycle on variation of hue with normalised temperature for wide-band crystal.

experiencing the first heating cycle. The data is shown in Figs. 9a and b, illustrating a difference in the hue–temperature characteristic for the heating and cooling cycles. In the cooling cycle, a decrease in the measured RGB values was observed (relative to the heating cycle) corresponding to a shift to a higher hue for the same measured surface temperature. The shift in hue is observed to be greatest for the 30 °C crystal; the magnitude of the shift was observed to increase with increasing maximum temperature before cooling, as also reported by Anderson and Baughn (2004). Once cooled below the activation temperature, the TLC resets and the subsequent heating cycle characteristic was generally reproduced within experimental uncertainty. However, this repeatability is limited by aging, as discussed in Section 3.5.

A similar hysteresis is observed for the wide-band crystal, as shown in Fig. 10a. Fig. 10b illustrates that the normalised temperature effectively collapses the wide-band data onto a single characteristic curve for both the heating and cooling cycles over a range $-1 < \zeta < 1$. The causes of hysteresis are complex and further investigation is required if a normalised temperature is to be usefully applied more universally.

Hysteresis can be reduced by ensuring that the calibrations are conducted in the same direction and from the same initial temperature as in the application, starting below or above the active colour–temperature range. In the application reported in Part 2, the transient method exposes a low temperature model to a heated flow and data is only collected in a heating cycle.

3.5. Aging and influence of film thickness

During each experiment the TLC experiences a heating cycle, where it is heated from 20 °C (below the activation temperature) to approximately 50 °C (well beyond the clearing-point) over a time of approximately 20 s. The TLC then cools to 20 °C before the next experiment. Typically one or two experiments were performed each day and it is important to assess if the *H–T* calibration is influenced by the aging inherent in this cyclic process. Wiberg and Lior (2004) reported that the thickness of the TLC layer affected the calibration and vulnerability to aging, i.e. a change in the hue–temperature relationship with time due to prolonged exposure to high temperature and use. Thicker layers of TLC were shown to be less sensitive to the effects of aging. Anderson and Baughn (2004) discuss a similar effect, reporting permanent damage to the TLC during exposure to temperatures above the clearing-point; the damage was characterised by a decrease in reflectivity and a shift in the temperatures at which the red and green intensity peaks were observed.

The above effects have all been observed in this study. The influence of film thickness (see discussion in Section 2.1) was investigated using the 30 °C crystal. Figs. 11a–c illustrate the variation of hue with temperature for 15, 30 and 45 μm film thicknesses, respectively, with the number of heating cycles used as a parameter – *C*1 is the first cycle, *C*5 the fifth, etc. Here each heating cycle takes the TLC from 20 to 32.5 °C (a temperature just beyond the clearing-point of the crystal) and then back to 20 °C, allowing the crystal to reset as it cools past the activation temperature

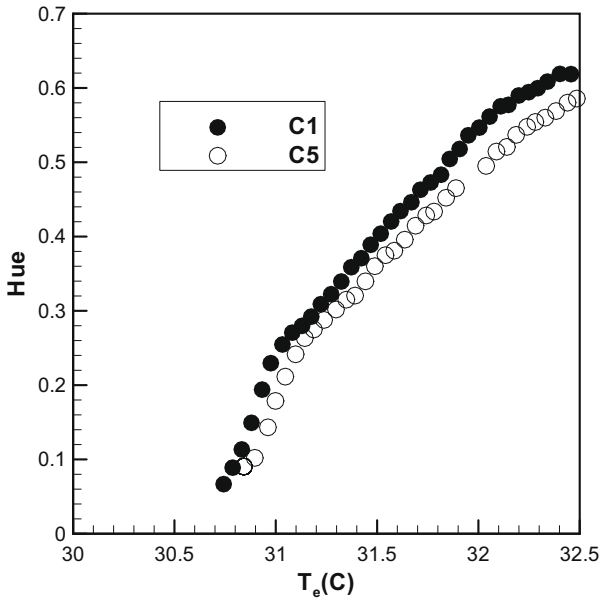

Fig. 11a. Effect of repeated heating cycles on variation of hue with temperature for 30 °C crystal with film thickness 15 μm.

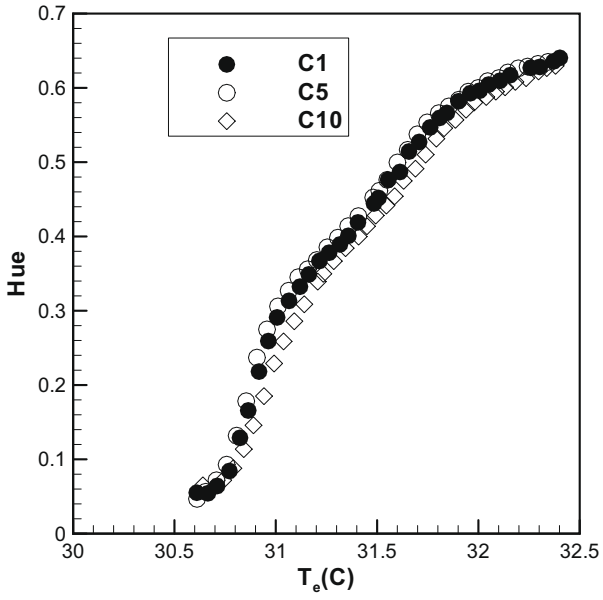

Fig. 11b. Effect of repeated heating cycles on variation of hue with temperature for 30 °C crystal with film thickness 30 μm.

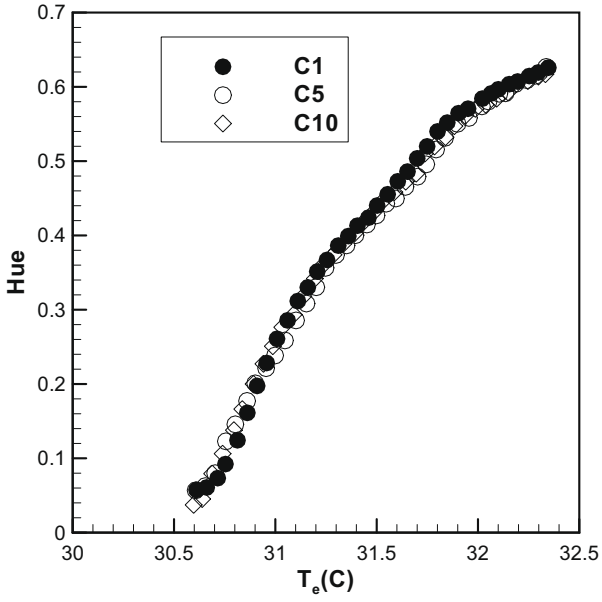

Fig. 11c. Effect of repeated heating cycles on variation of hue with temperature for 30 °C crystal with film thickness 45 μm.

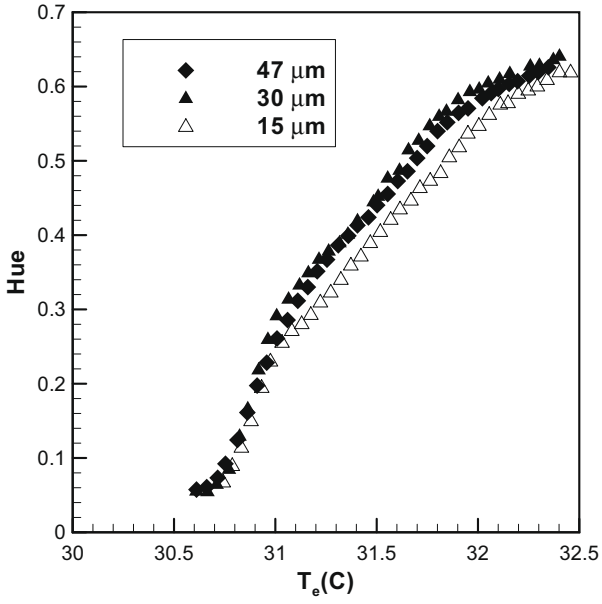

Fig. 11d. Effect of film thickness on variation of hue with temperature for 30 °C crystal for first heated cycle.

(~30.5 °C). Hysteresis occurs but only data for the heating portion of the cycle is shown.

The data illustrates that the hue–temperature relationship of the thinner films changes as the TLC is cycled past the clearing-point. For a fixed temperature, the curves are observed to shift to a lower hue as the number of cycles increase; as discussed below in reference to Fig. 13, there is a corresponding shift in the peak *R* and *G* intensity levels and their associated temperatures in this aging process. The thinnest film is shown to be most sensitive to aging; the calibration of the thickest film (45 μm) is shown not to be influenced significantly up to 10 cycles. Fig. 11d is a plot of *H* versus *T* for the three film thicknesses for the first heating cycle, illustrating that the crystal calibration depends upon the thickness of the layer even before aging occurs. The differences in the calibration are much smaller for the two thicker films, and it is important to note that any non-uniformity in film thickness may cause errors in the measured temperature.

One probable cause of aging is the exposure to ultra-violet (UV) radiation. However, in the aging experiments reported here, an indirect view was used, and the polycarbonate would have acted as an effective filter for the UV light from the strobe. It is possible that the more rapid aging of thin films of TLC, which has been noted by others for the direct view case, was caused – or increased – by the absorption of UV radiation by the exposed outer layers of crystal; for thick films, the outer layers might act as a UV filter, protecting the inner layers from the aging process. The fact that aging also occurs for the indirect view case, where UV effects are thought to be negligible, suggests that some other mechanism might be responsible. More work is needed before a definitive reason can be given for the cause of TLC aging.

As observed by others, the crystals also age when exposed to high temperature for a significant period of time. The sensitivity to aging and damage (a permanent decrease in reflected intensity) is shown to be more acute for thinner films. This was demonstrated by heating the 30 °C crystal from 20 to 60 °C (curve denoted *C*1 in Figs. 12a–c) and holding the crystal at this maximum temperature for 150 min before cooling to 20 °C; the crystal is subsequently heated through its active range (curve denoted *C*2 in Figs. 12a–c. Fig. 12a illustrates the variation of *H* with *T* for a film thickness of 15 μm and it is observed that for a given temperature there is

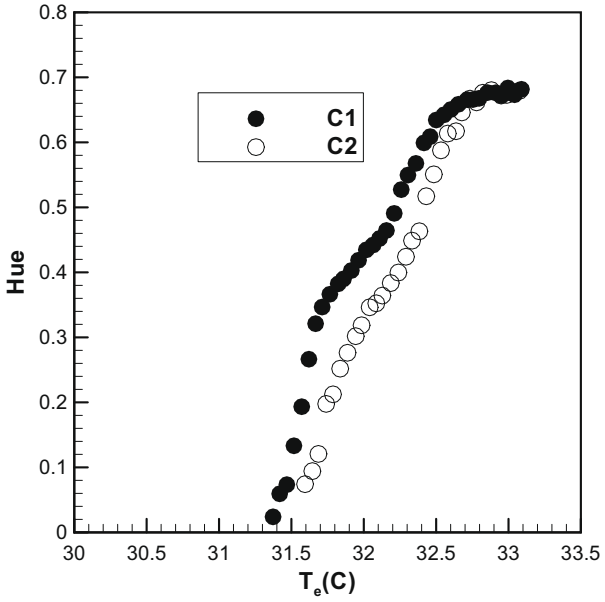

Fig. 12a. Effect of exposure to high temperature for 30 °C crystal with film thickness 15 μm.

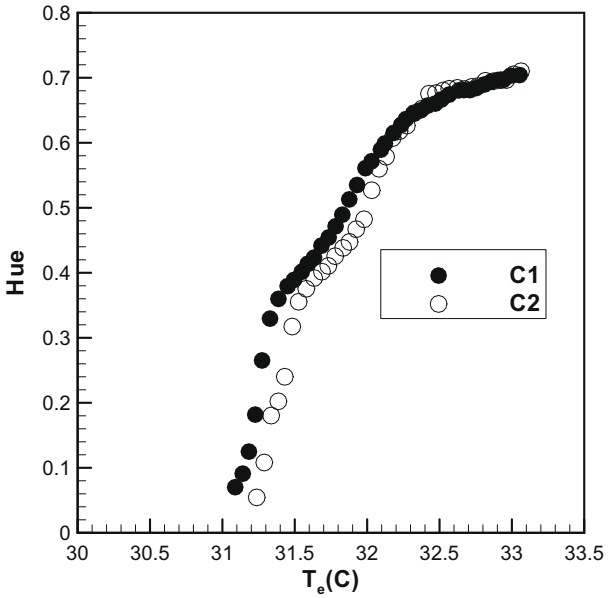

Fig. 12b. Effect of exposure to high temperature for 30 °C crystal with film thickness 30 μm.

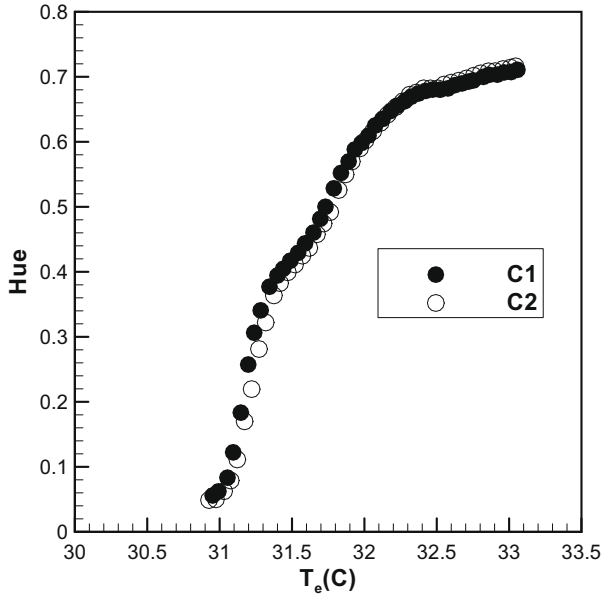

Fig. 12c. Effect of exposure to high temperature for 30 °C crystal with film thickness 45 μm.

a significant shift to a lower hue in the second cycle. This shift in the TLC colour–temperature relationship is more marked than that observed in the data in Fig. 11a, which corresponded to a significantly less exposure beyond the clearing-point temperature and a lower peak exposure temperature (32.5 versus 60 °C) prior to cooling. Similar data for the 30 and 45 μm film thicknesses are shown in Figs. 12b and c, where the aging effect is shown to be less pronounced. The shift in hue between the two cycles is related to deterioration in the visibility of the TLC (i.e. a reduction in the reflected intensity) as well as a shift in the temperature of the peak *R* and *G* maxima.

Figs. 13a and b shows the *R* and *G* intensities versus temperature for the 30 and 45 μm TLC film thicknesses for the two heating cycles, *C*1 and *C*2, corresponding to the hue data presented in Figs.

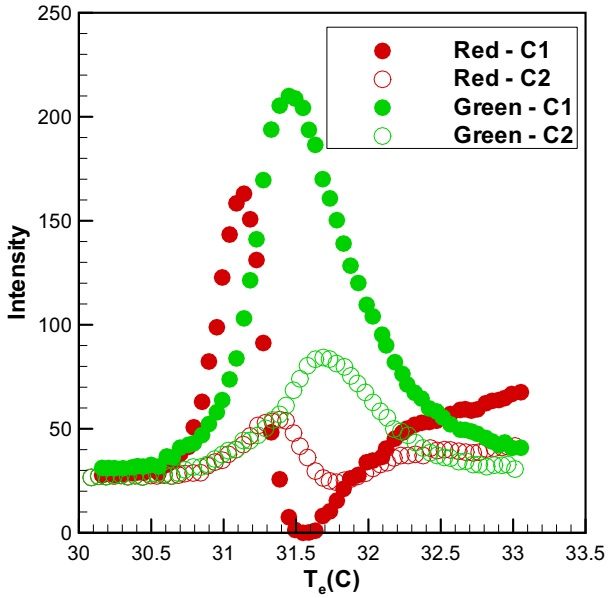

Fig. 13a. Effect of exposure to high temperature for 30 °C crystal with film thickness 30 μm.

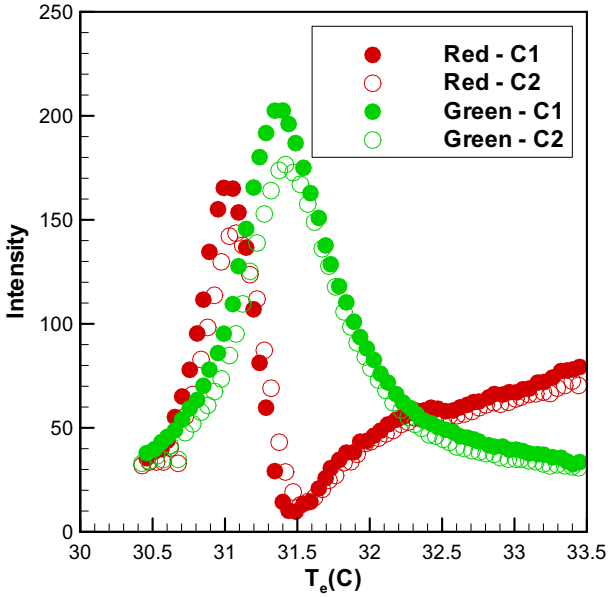

Fig. 13b. Effect of exposure to high temperature for 30 °C crystal with film thickness 45 μm.

12b and c, respectively. Data for the green intensity is tabulated in more detail in Table 1. The aging has reduced the G intensity of the 30 μm film by 60% where the deterioration in visibility is so acute the crystal can no longer be used effectively. The *H–T* relationship for the 45 μm film has been essentially preserved between cycles *C*1 and *C*2 though the peak G intensity has been reduced by 13%. These aging experiments, with their associated measurements of peak *R* and *G* intensities, provide a useful measure of the fidelity of the TLC calibration.

3.6. Summary of the calibration

The experimental application (see Part 2) uses the 30 and 40 °C crystals with an indirect view, lighting angle of 34°, heating (rather than cooling) direction, and film thickness of 45 μm. With reference to the experiments, these calibrations were not *in situ* but they do account for the lighting arrangements, optical path, heating and cooling cycles, and peak temperatures experienced by the TLC on the experimental apparatus. In all experimental cases the time of exposure to high temperature was significantly less than the extremes tested in the calibrations, and the number of heating cycles experienced by the TLC never created a measureable deterioration in the peak *R* and *G* intensities. While of practical importance, the reported TLC calibrations are limited in the sense that they are applicable to the specific experimental arrangement used. However, the range of this investigation has provided insight into the importance and influence of the various factors governing any general calibration.

Table 1
Reduction in peak green intensity due to aging.

Green intensity					
Thickness (μm)	Cycle	*T*	Hue	Peak intensity	% Reduction
30	*C*1	31.4	0.38	210	
	*C*2	31.7	0.4	84	60
45	*C*1	31.4	0.39	202	
	*C*2	31.1	0.38	176	13

4. Conclusions

An extensive set of calibrations for wide-band and narrow-band TLC has been reported, with the colour response presented as a hue–temperature relationship. An apparatus was designed to account for both direct and indirect (through polycarbonate) views of the TLC on an isothermal surface of known temperature. The two calibrations were shown to have a similar shape and activation range in terms of hue and temperature. However, as stated above, the indirect view (which modelled the experimental arrangement) produced a shift in the hue–temperature relationship.

Narrow-band crystals were observed not to be significantly affected by variations in viewing angle between 20° and 45°, provided the hue did not exceed the green-to-blue transition ($H \sim 0.38$). In contrast, the calibration of the wide-band TLC featured a significant shift in hue with viewing angle over the entire active range of the crystal. A normalised temperature was shown to effectively collapse the wide-band data onto a single characteristic curve, simplifying the quantitative response of the wide-band TLC over the range of lighting conditions and viewing angles tested.

All TLC exhibited similar hysteresis behaviour when cooled after being heated, provided the final temperature in a calibration cycle was high enough relative to the activation range. In the cooling cycle, a decrease in the measured RGB values was observed (relative to the heating cycle), corresponding to a shift to a higher hue for the same measured surface temperature. The magnitude of the effect was observed to increase with increasing maximum temperature before cooling. Once cooled below the lower activation temperature, the TLC resets and the heating cycle characteristic was generally reproduced unless influenced by aging effects.

In heat transfer experiments, the film should be sufficiently thin that TLC temperature is (within reason) the same as the surface temperature of a semi-infinite substrate and subject to the same heat transfer history. The thickness of the TLC layer has been shown to affect the calibration and the vulnerability to aging, i.e. a change in the hue–temperature relationship with time due to prolonged exposure to high temperature and use. Permanent damage to the TLC, characterised by a decrease in reflectivity and a shift in the temperatures at which the red and green intensity peaks were observed, occurred during exposure to temperatures above

the clearing-point. The sensitivity to aging and damage is shown to be more acute for thinner film thicknesses.

The generic calibrations substantiate the findings of others and provide new insights into how important effects (especially aging, TLC film thickness, 'optical path' and the use of a normalised temperature) influence the various factors governing the hue–temperature relationship. The 30 and 40 °C narrow-band TLC were also specifically calibrated for application to a transient experiment modelling the flow of internal cooling in a gas turbine, as presented in Part 2.

Acknowledgement

Dr. James Mayhew participated in this research while on sabbatical from Rose-Hullman Institute of Technology between September 2006 and March 2007.

References

Anderson, M.R., Baughn, J.W., 2004. Hysteresis in liquid crystal thermography. ASME J. Heat Transf. 126, 339–346.

Anderson, M.R., Baughn, J.W., 2005. Liquid crystal thermography: illumination spectral effects. Part 1 – experiments. ASME J Heat Transf. 127, 581–587.

Bahadur, B., 1998. Liquid Crystal Application and Uses, vol. 7. World Scientific, Singapore.

Baughn, J.W., Anderson, M.R., Mayhew, J.E., Wolf, J.D., 1999. Hysteresis of thermochromic liquid crystal temperature measurement based on hue. ASME J. Heat Transf. 121, 1067–1072.

Behle, M., Schultz, K., Leiner, W., Fiebig, M., 1996. Color-based image processing to measure local temperature distributions by wide-band liquid crystal thermography. Appl. Sci. Res. 56 (2), 113–143.

Camci, C., Kim, K., Hippensteele, S.A., 1992. A new hue-capturing technique for the quantitative interpretation of liquid crystal images used in convective heat transfer studies. ASME J. Turbomach. 114, 765–775.

Camci, C., Glezer, B., Owen, J.M., Pilbrow, R.G., Syson, B.J., 1998. Application of themochromic liquid crystal to rotating surfaces. ASME J. Turbomach. 120, 100–103.

Chan, T.L., Ashforth-Frost, S., Jambunatahan, K., 2001. Calibrating for viewing angle effect during heat transfer experiments on a curved surface. ASME Int. J. Heat. Mass. Transf. 44, 2209–2223.

Farina, D.J., Hacker, J.M., Moffat, R.J., Eaton, J.K., 1994. Illuminant invariant calibration of thermochromic liquid crystals. Exp. Therm. Fluid Sci. 9 (1), 1–12.

Hay, J.L., Hollingsworth, D.K., 1998. Calibration of micro-encapsulated liquid crystals using hue angle and a dimensionless temperature. J. Exp. Therm. Fluid Sci. 18, 251–257.

Ireland, P.T., Jones, T.V., 1986. Detailed measurements of heat transfer on or around a pedestal in fully developed passage flow. In: Eighth International Heat Transfer Conference, vol. 3, pp. 975–980.

Ireland, P.T., Jones, T.V., 2000. Liquid crystal measurements of heat transfer and surface shear stress. Meas. Sci. Technol. 11, 969–986.

Kasagi, N., Moffat, R.J., Hirata, M., 1989. Liquid crystals. In: Yan, Wen Jel (Ed.), Handbook of Flow Visualization. Hemisphere, New York (Chapter 8).

Sabatino, D.R., Praisner, T.J., Smith, C.R., 2000. A high-accuracy calibration technique for thermochromic liquid crystal temperature measurements. J. Exp. Fluids 28, 497–505.

Syson, B.J., Pilbrow, R.G., Owen, J.M., 1996. Effect of rotation on temperature response of thermochromic liquid crystal. Int. J. Heat Fluid Flow 17, 491–499.

Wiberg, R., Lior, N., 2004. Errors in Thermochromic Liquid Crystal Thermometry. Rev. Sci. Instrum. 75 (9), 2985–2994.